

## **Phosphorene Nanoribbons, Phosphorus Nanotubes and van der Waals Multilayers**

*Hongyan Guo<sup>1,2,⊥</sup>, Ning Lu<sup>3,2,⊥</sup>, Jun Dai<sup>2</sup>, Xiaojun Wu<sup>1,4,5\*</sup>, Xiao Cheng Zeng<sup>2,4,\*</sup>*

<sup>1</sup>CAS Key Lab of Materials for Energy Conversion, Department of Materials Science and Engineering, University of Science and Technology of China, Hefei, Anhui 230026, China, <sup>2</sup>Department of Chemistry and Department Mechanics and Materials Engineering, University of Nebraska-Lincoln, Lincoln, NE 68588, USA, <sup>3</sup>Center for Nano Science and Technology, Department of Physics, Anhui Normal University, Wuhu, Anhui 241000, China, <sup>4</sup>Hefei National Laboratory for Physical Sciences at the Microscale, University of Science and Technology of China, Hefei, Anhui 230026, China, <sup>5</sup>Synergetic Innovation Center of Quantum Information & Quantum Physics, University of Science and Technology of China, Hefei, Anhui 230026, China

<sup>⊥</sup> Both authors contribute equally to this work.

\*Email: xzeng1@unl.edu; xjwu@ustc.edu.cn

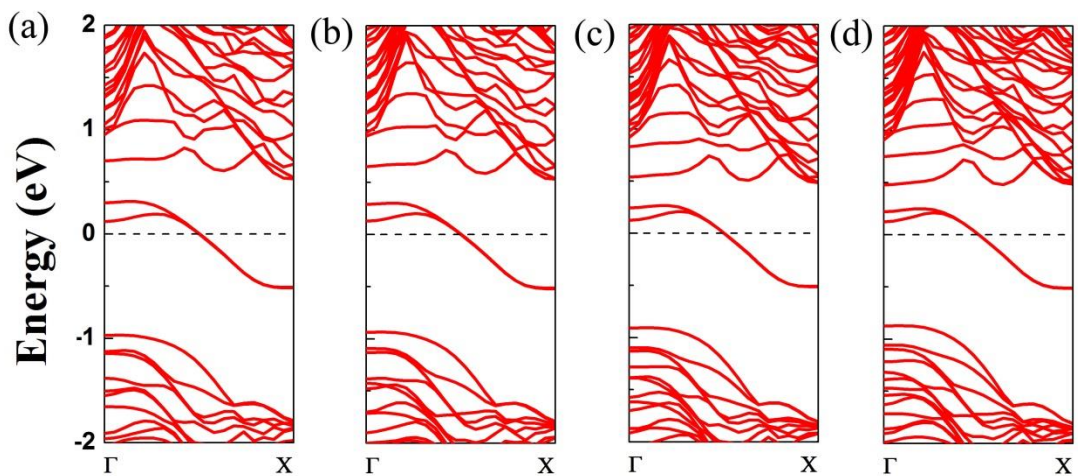


**Figure S1.** Computed band structures (PBE) of the edge-unpassivated (a) 7-, (b) 8-, (c) 9-, (d) 10-z-PNRs. The Fermi level is set to zero.

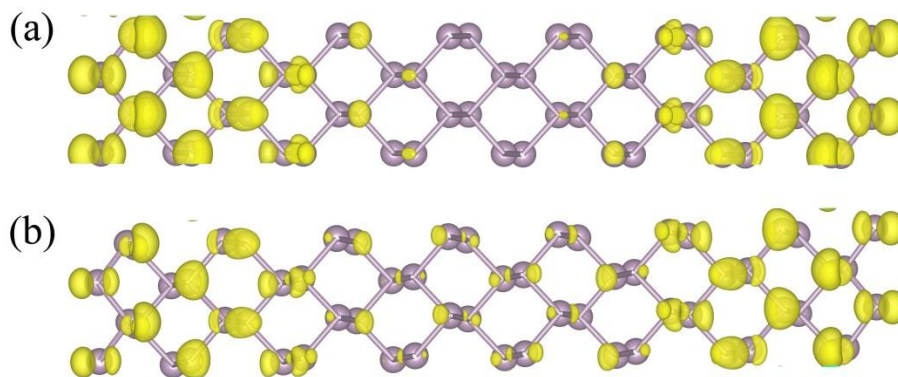


**Figure S2.** The partial charge density distribution corresponding to (a)  $\alpha$  and (b)  $\beta$  band at the  $\Gamma$  point, respectively, for the edge-unpassivated 8-z-PNR.

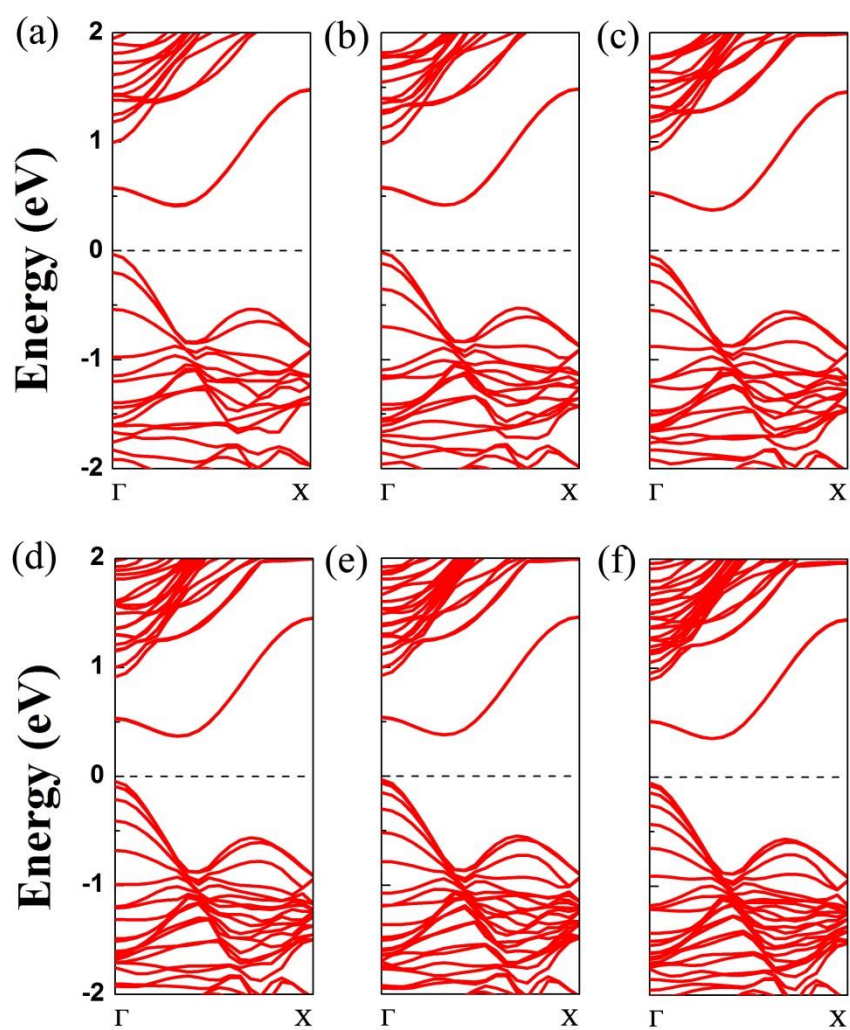


**Figure S3.** Computed band structures (PBE) of the edge-unpassivated (a) 7-, (b) 8-, (c) 9-, (d) 10-, (e) 11-, and (f) 12-*a*-PNRs. The Fermi level is set to zero.

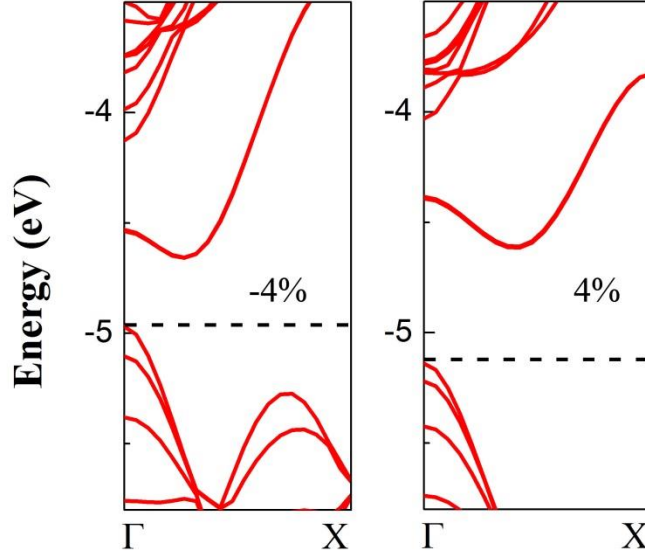


**Figure S4.** Computed band structures (PBE) of the edge-unpassivated 8-*a*-PNR at the strain of -4% and 4%. The vacuum level is set to zero. The dashed line denotes the Fermi level.

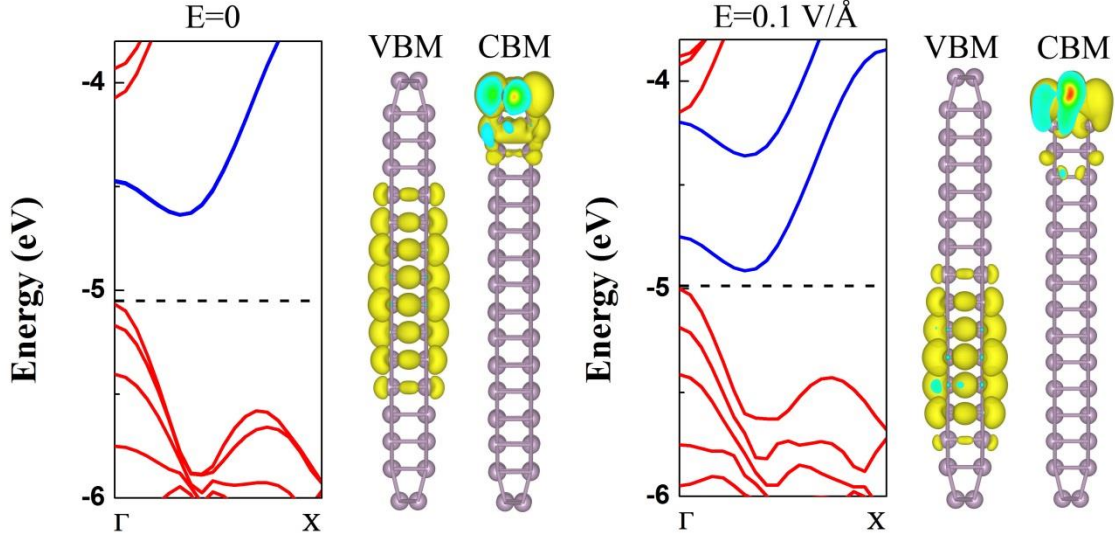


**Figure S5.** Computed band structures (PBE) and partial charge density distribution corresponding to the VBM and CBM for the edge-unpassivated 8-*a*-PNR at zero and an external in-plane transverse electric field of 0.1 V/Å, respectively. The vacuum level is set to zero. The dashed line denotes the Fermi level. The CBM corresponds to the edge-state and the corresponding bands are highlighted by blue lines.

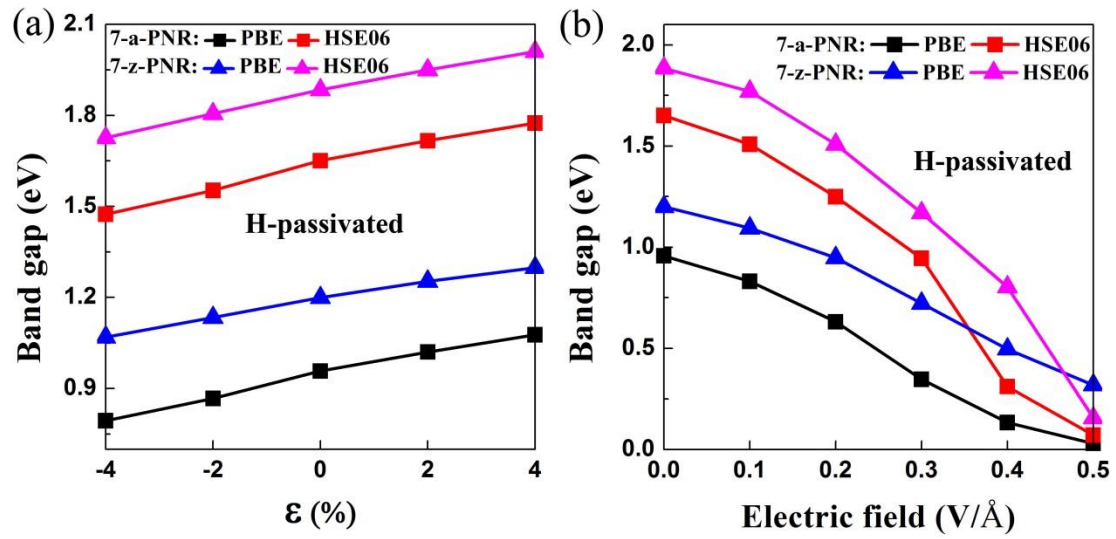


**Figure S6.** (a) Computed bandgaps of the edge-passivated 7-*a*-PNR and 7-*z*-PNR by hydrogen *versus* the tensile strain, ranging from -4% to 4%, “-” represents compression and “+” represents expansion. (b) Computed bandgaps *versus* in-plane transverse electric field for the edge-passivated 7-*a*-PNR and 7-*z*-PNR.

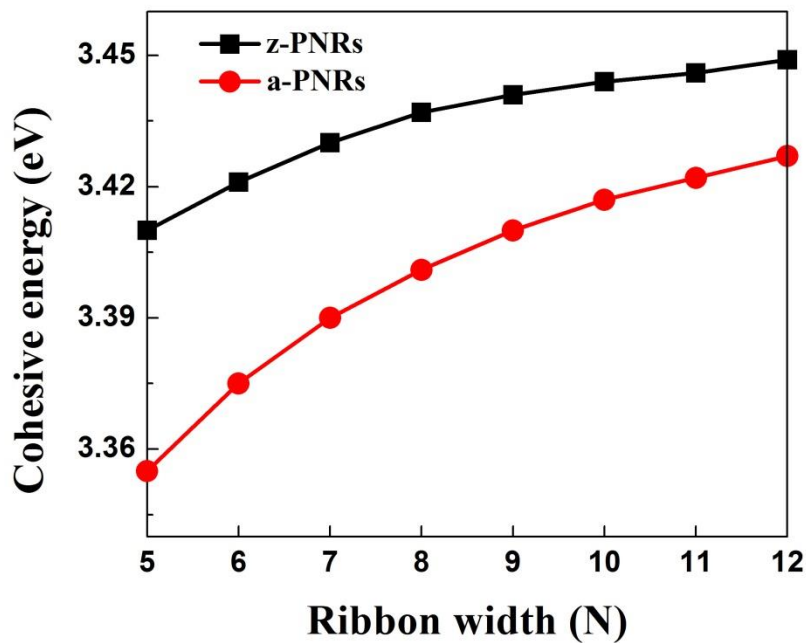


**Figure S7.** Computed cohesive energy per atom of the edge-unpassivated PNRs *versus* the ribbon width  $N$  ( $5 \leq N \leq 12$ ).

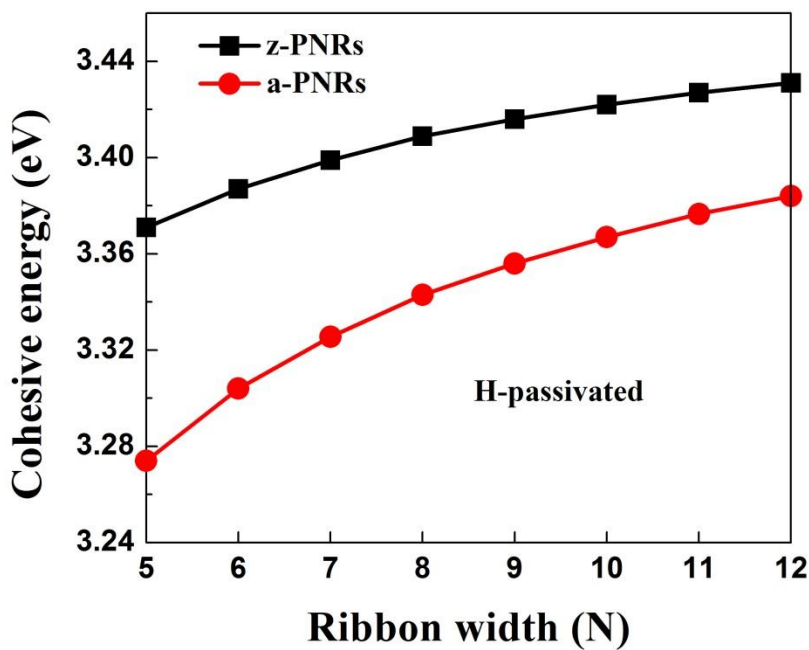


**Figure S8.** Computed cohesive energy per atom of the edge-passivated PNRs *versus* the ribbon width ( $5 \leq N \leq 12$ ).



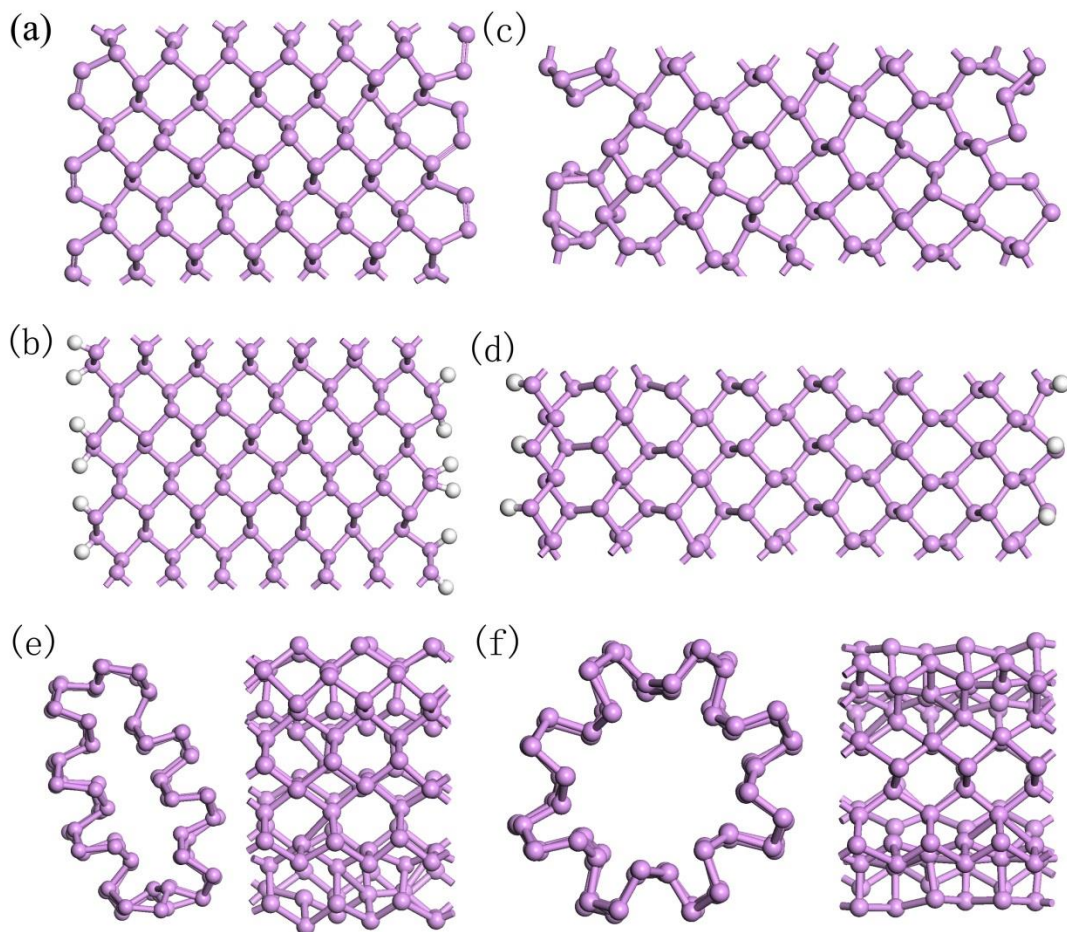


**Figure S9.** Snapshots of BOMD simulations at 8 ps for (a) the edge-unpassivated 7-*a*-PNR, (b) the edge H-passivated 7-*a*-PNR, (c) the edge-unpassivated 7-*z*-PNR, and (d) the edge H-passivated 7-*z*-PNR, as well as at 8 ps for (e) the armchair PNT (0, 8) [top view on the left and side view on the right], all with temperature controlled at 600 K. A snapshot of BOMD simulation at 8 ps for (f) the armchair PNT (0, 8) [top view on the left and side view on the right], with temperature controlled at 400 K.

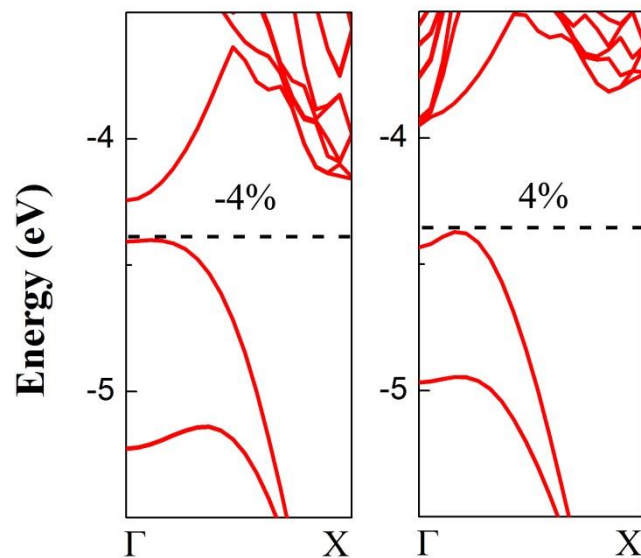


**Figure S10.** Computed band structures (PBE) of armchair PNT (0, 8) at strain of -4% and 4%. The vacuum level is set to zero. The dashed line denotes the Fermi level.

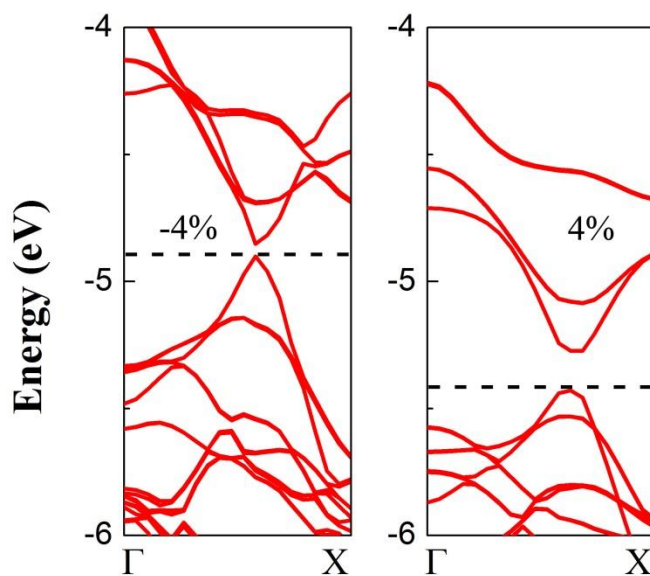


**Figure S11.** Computed band structures (PBE) of zigzag PNT (12, 0) at strain of -4% and 4%. The vacuum level is set to zero. The dashed line denotes the Fermi level.



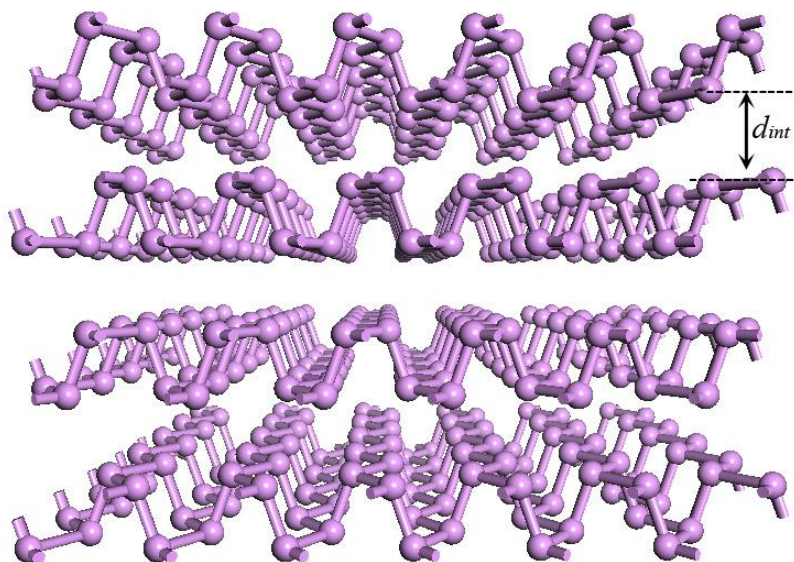


**Figure S12.** Geometric structure of multilayer phosphorene.  $d_{int}$  represents the interlayer spacing between two adjacent phosphorene monolayers.

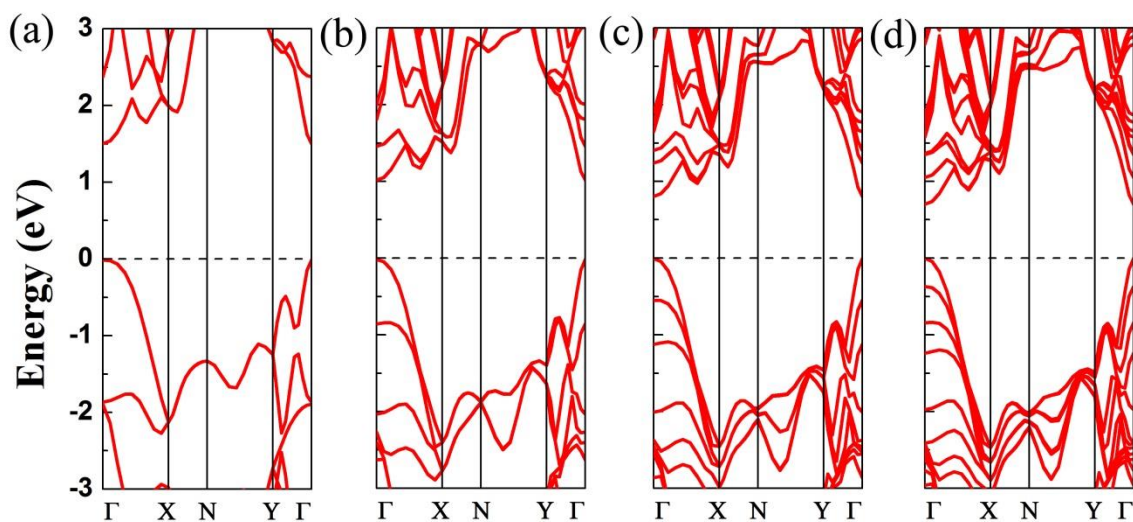


**Figure S13.** Computed band structures (HSE06) of (a) monolayer, (b) bilayer, (c) trilayer, (d) 4-layer phosphorene sheets. The Fermi level is set to zero.

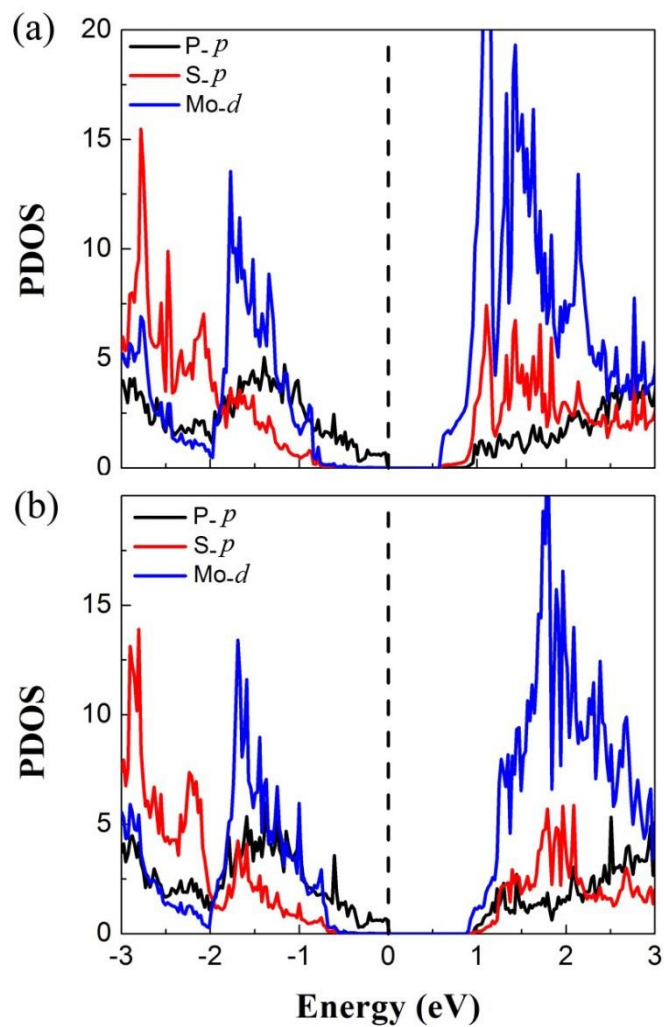


**Figure S14.** Computed partial density of states (PDOS) of (a) MoS<sub>2</sub>/phosphorene and (b) WS<sub>2</sub>/phosphorene heterobilayers. The Fermi level is set to zero.

**Table S1:** Cell parameter  $a_1$  and  $a_2$  (in Å) of multilayer phosphorene and the interlayer spacing between two adjacent phosphorene layers  $d_{int}$  (in Å).

	$a_1$	$a_2$	$d_{int}$
Monolayer	3.32	4.58	/
Bilayer	3.33	4.52	3.18
Trilayer	3.34	4.50	3.22
4-layer	3.34	4.50	3.23

**Table S2.** The charge transfer  $q$  (in unit of  $e$ ) between the MoS<sub>2</sub> (or WS<sub>2</sub>) and phosphorene layers with and without the electric field  $E$  (in V/ Å).

$E$	0	0.2	0.4
$q$ (MoS <sub>2</sub> /phosphorene)	0.1	0.15	0.2
$q$ (WS <sub>2</sub> /phosphorene)	0.07	0.11	0.15